Contrast source inversion on experimental data
Initial results

Taskin, Ulas; Suzuki, Atsuro; Terada, Takahide; Tsubota, Yushi; Dongen, Koen W.A.Van

DOI
10.1117/12.2610972

Publication date
2022

Document Version
Final published version

Published in
Medical Imaging 2022

Contrast source inversion on experimental data: initial results

Ulas Taskin, Atsuro Suzuki, Takahide Terada, Yushi Tsubota, Koen W. van Dongen

Ulas Taskin, Atsuro Suzuki, Takahide Terada, Yushi Tsubota, Koen W. A. van Dongen, "Contrast source inversion on experimental data: initial results," Proc. SPIE 12038, Medical Imaging 2022: Ultrasonic Imaging and Tomography, 120380T (4 April 2022); doi: 10.1117/12.2610972

SPIE.

Event: SPIE Medical Imaging, 2022, San Diego, California, United States

Contrast source inversion on experimental data: initial results

Ulas Taskin[a, c], Atsuro Suzuki[b], Takahide Terada[b], Yushi Tsubota[b], and Koen W. A. van Dongen[a]

[a]Department of Imaging Physics, Delft University of Technology, 2628 CJ, Delft, the Netherlands
[b]Innovative Technology Laboratory, FUJIFILM Healthcare Corporation, Japan
[c]Openwater, USA

ABSTRACT

Quantitative images showing the speed of sound profile of the breast may be obtained by employing full-waveform inversion (FWI) methods on the measured data. These reconstruction methods work well for both dense and normal breasts. Contrast source inversion (CSI) is a frequency domain FWI method. In literature, many examples of successful application of CSI for breast imaging can be found. However, all these works are based on simulated data. In this work, we will present our first results obtained with employing CSI on experimental data. CSI was developed by Delft University of Technology and the experimental data was provided by FUJIFILM Healthcare Corporation. The experimental data is obtained using a ring-shaped transducer which scans a breast-mimicking gelatine phantom. Our initial results obtained with CSI look promising; all inclusions within the phantom are accurately reconstructed.

Keywords: breast ultrasound, contrast source inversion, full-wave inversion

1. INTRODUCTION

Breast cancer is the most common type of cancer among women.[1] Many studies have shown that early detection and early diagnosis aid to an increase in the overall survival rate.[2] For this reason, national screening programs using mammography have been introduced in the past.[3] However, mammography has several drawbacks such as a low sensitivity with dense breasts.[4] This drawback is of great importance since breast density is a well-known risk factor.[5] This problem could be avoided by using ultrasound as a screening modality. Moreover, ultrasound is known to work well with dense breasts as well as that the acoustic properties of the tumour deviate significantly from the surrounding healthy tissue. These observations have resulted in the development of ultrasonic water bath scanning systems. With these systems tomographic scans of the breast are made. Some of these systems have already been tested in a clinical setting.[6–8] With a water bath scanner, the breast is scanned from all sides, and transmission and reflection measurements are done simultaneously. From this data, three kind of images can be generated; reflectivity, speed of sound, and attenuation images. Reflectivity images reveal information about the echogenicity of breast tissues, whereas, speed of sound and attenuation images provide quantitative acoustical material properties of the breast tissues. Consequently, in the ideal case, tissue characterization and cancer diagnosis are done by combining these three images.[9]

It is known that full-wave inversion methods (FWI) are the best imaging methods to generate accurate speed-of-sound images.[10] FWI methods account for most wave phenomena during the reconstruction at the cost of a high computational complexity due to the non-linearity. Fortunately, FWI methods have the advantage that they may reconstruct high-resolution images containing quantitative information about the tissue parameters. The FWI method used in this work – contrast source inversion (CSI) – is based on solving the scattering integral equation and works in the frequency domain.[11] Most other FWI methods are based on time-domain finite-difference modeling methods. These time-domain methods usually require a denser spatial sampling as compared to the scattering integral based methods in order to satisfy the Courant condition and to avoid effects

Further author information: (Send correspondence to U.T.)
U.T.: E-mail: u.taskin@tudelft.nl
K.W.A.D.: E-mail: K.W.A.vanDongen@tudelft.nl

Medical Imaging 2022: Ultrasonic Imaging and Tomography, edited by Nick Bottenus, Nicole V. Ruiter,
Proc. of SPIE Vol. 12038, 120380T · © 2022 SPIE · 1605-7422 · doi: 10.1117/12.2610972

such as numerical dispersion. In addition, for the frequency-domain methods only a few frequency components are usually sufficient to conduct the inversion, which makes CSI computationally attractive.[12–14]

In this work, we investigate the application of CSI on a real measurement. Measurement data is acquired from a circular setup that is built by FUJIFILM Healthcare Corporation.[15,16] The paper is organized as follows. In section 2, the theory behind CSI is explained briefly. Please refer to the cited literature for an extensive explanation of CSI.[17] In section 3, initial results obtained with CSI is presented. In section 4, a conclusion and future direction of the work is given.

2. THEORY

In this work CSI is used as a frequency domain two-dimensional FWI method. With CSI, the inversion procedure consist of minimizing the object and data equations which read

$$\hat{p}(\boldsymbol{x}) = \hat{p}^{\mathrm{inc}}(\boldsymbol{x}) + \omega^2 \int_{\mathbb{D}} \hat{G}(|\boldsymbol{x} - \boldsymbol{x}'|)\hat{w}(\boldsymbol{x}')dA(\boldsymbol{x}'), \quad \boldsymbol{x} \in \mathbb{D}, \tag{1}$$

and

$$\hat{p}^{\mathrm{sct}}(\boldsymbol{x}) = \omega^2 \int_{\mathbb{D}} \hat{G}(|\boldsymbol{x} - \boldsymbol{x}'|)\hat{w}(\boldsymbol{x}')dA(\boldsymbol{x}'), \quad \boldsymbol{x} \in \mathbb{S}, \tag{2}$$

where $\hat{p}(\boldsymbol{x})$, $\hat{p}^{\mathrm{inc}}(\boldsymbol{x})$, and $\hat{p}^{\mathrm{sct}}(\boldsymbol{x})$ are the total, incident and scattered pressure fields respectively; $\boldsymbol{x}$ denotes a position in $\mathbb{R}^2$; $\mathbb{D}$ is the spatial domain that includes the object and that is enclosed by the boundary $\mathbb{S}$; ω is the angular frequency; $\hat{G}(|\boldsymbol{x} - \boldsymbol{x}'|)$ is the Green's function for the homogeneous embedding; $\hat{w}(\boldsymbol{x}')$ is the contrast source that is defined as

$$\hat{w}(\boldsymbol{x}') = \chi(\boldsymbol{x}')\hat{p}(\boldsymbol{x}'), \tag{3}$$

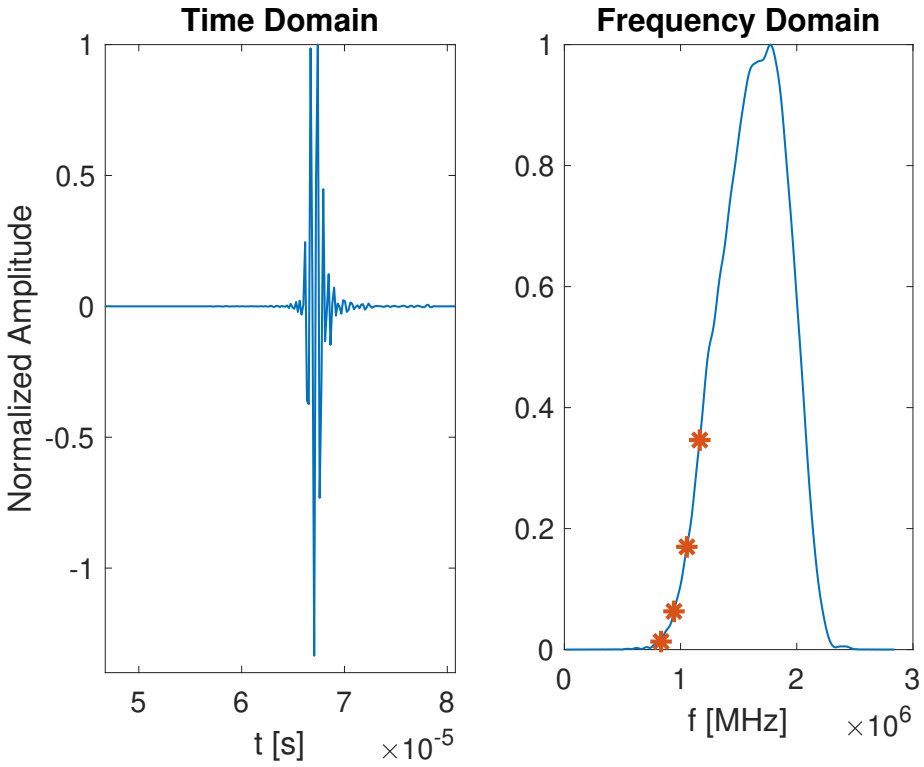

Figure 1. Source excitation profile in time (left) and frequency (right) domain. The red asterisks indicate the four frequency components used in CSI.

where $\chi(\boldsymbol{x}')$ is the contrast function that reads

$$\chi(\boldsymbol{x}') = \frac{1}{c^2(\boldsymbol{x}')} - \frac{1}{c_0^2}, \tag{4}$$

where $c(\boldsymbol{x}')$ and c_0 are the speed of sound of the medium and the homogeneous embedding respectively. In this work, it is assumed that the mass density $\rho(\boldsymbol{x}')$ is constant in the whole medium. However, it is also possible to reconstruct both speed of sound and density profiles accurately[18] with the aid of the redatuming methods earlier developed.[19,20]

With CSI, the unknown contrast source is updated using an iterative scheme that minimizes the cost function E that equals

$$E = \eta_{\mathbb{S}} \|\hat{p}^{\text{sct}} - \mathrm{L}^{\mathbb{S}}[\hat{w}]\|_{\mathbb{S}}^2 + \eta_{\mathbb{D}} \|\chi \hat{p}^{\text{inc}} - w + \chi \mathrm{L}^{\mathbb{D}}[\hat{w}]\|_{\mathbb{D}}^2, \tag{5}$$

where $\eta_{\mathbb{S}}$ and $\eta_{\mathbb{D}}$ are normalization terms, and where $\mathrm{L}^{\mathbb{D}}$ and $\mathrm{L}^{\mathbb{S}}$ are integral operators derived from equations (1) and (2), respectively.

In the conventional implementation of CSI the cost function E is minimized for a limited number of frequency components simultaneously. That might be problematic when the cycle skipping for the higher frequency components is dominating the inversion process. To avoid cycle skipping, frequency hopping is used frequently. Since CSI works in the frequency domain, frequency hopping implementation is straightforward. With the frequency hopping implemented, CSI is started with the lowest frequency component only. The reconstructed contrast source term for this frequency component inversion is successively used as a starting model for the next frequency component. Continuing this way, all the selected frequency components are used for the inversion sequentially. Having already a good starting model for the higher frequency components helps to reduce artefacts in the image due to cycle skipping. In this way high resolution reconstructions may be obtained.[21]

3. RESULTS

3.1 Measurement setup

The employed measurement setup includes a 1024 element circular array transducer with a radius of 5 cm and an element pitch of 0.3 mm. The center frequency of the system is around 1.69 MHz. The source excitation profile is shown in Figure 1. Our initial inversion result is obtained using the four frequency components indicated by the red asterisks. Those four components are selected from the lower part of the available bandwidth to avoid cycle-skipping problems. Measured data is acquired using the oil-gel based breast mimicking phantom shown in Figure 2. The phantom has a diameter of 51 mm and contains four inclusions with diameters varying from 3 mm up to 10 mm.

A full measurement consist of 128 source locations equally distributed along the circle. For each excitation of the source, the pressure field is measured by 768 receiving elements equally distributed along the circle. Note that, for CSI it is advantageous to have more receivers than sources.[22] An example of the raw data for a measurement in water is shown in Figure 3. Note that, the signal is heavily distorted by noise before 2.3 μs and after 8 μs. That's why those parts are removed from the data and not used during reconstruction.

3.2 Reconstruction

CSI results using the four frequency components (see Figure 1) after 256 iteration is shown in Figure 4. All four inclusions are clearly visible in the reconstructed speed of sound profile. For this measurement, the phantom is placed in water and the inclusions in the phantom are filled with salty water. The temperature is $25°C$. At this temperature, the oil-gel phantom has a lower speed of sound then the water, whereas the salty water has higher speed of sound then the water.[16] Our reconstruction result is in agreement with this information. It can be seen from the reconstructed image that the inclusions are brighter which indicates higher speed of sound values, while the phantom itself is darker which indicates a lower speed of sound value.

The reconstruction shown in Figure 4 is not perfect as a final result. However, we believe that it is quite promising as an initial result. Note that this image is obtained using only a limited part of the available data. It is expected that the reconstructed image will improve by using more data. For example, the noise in the

background can be suppressed by using more frequency components during the inversion at the cost of an increase in computing time. Additional improvements may be achieved by using a different starting model[23] or by using advanced pre-processing and optimization/regularization methods.[18–20,24,25]

4. CONCLUSION

Contrast source inversion (CSI) is applied on experimental data acquired with a realistic measurement setup. Promising initial reconstruction results have been obtained by processing the measured data with CSI. It is expected that these results will improve by increasing the number of sources or frequency components.

In this work, we only show initial result of CSI for a realistic measurement setup. A full reconstruction that includes all data and uses advanced (pre)-processing, optimization and regularization methods is left for future work. With a full reconstruction, a comparison with other FWI methods can be made as well.

REFERENCES

[1] Bray, F., Ferlay, J., Soerjomataram, I., Siegel, R. L., Torre, L. A., and Jemal, A., "Global cancer statistics 2018: Globocan estimates of incidence and mortality worldwide for 36 cancers in 185 countries," *CA: a cancer journal for clinicians* **68**(6), 394–424 (2018).

[2] Carioli, G., Malvezzi, M., Rodriguez, T., Bertuccio, P., Negri, E., and La Vecchia, C., "Trends and predictions to 2020 in breast cancer mortality in europe," *The Breast* **36**, 89–95 (2017).

[3] RIVM, "Breast cancer in the netherlands." https://www.rivm.nl/en/breast-cancer-screening-programme/breast-cancer-in-netherlands. Accessed: 2021-10-24.

[4] Guo, R., Lu, G., Qin, B., and Fei, B., "Ultrasound imaging technologies for breast cancer detection and management: a review," *Ultrasound in Medicine & Biology* **44**(1), 37–70 (2018).

[5] Boyd, N. F., Guo, H., Martin, L. J., Sun, L., Stone, J., Fishell, E., Jong, R. A., Hislop, G., Chiarelli, A., Minkin, S., et al., "Mammographic density and the risk and detection of breast cancer," *New England Journal of Medicine* **356**(3), 227–236 (2007).

[6] Hopp, T., Zapf, M., Kretzek, E., Henrich, J., Tukalo, A., Gemmeke, H., Kaiser, C., Knaudt, J., and Ruiter, N. V., "3d ultrasound computer tomography: update from a clinical study," in [*Medical Imaging 2016: Ultrasonic Imaging and Tomography*], **9790**, 97900A, International Society for Optics and Photonics (2016).

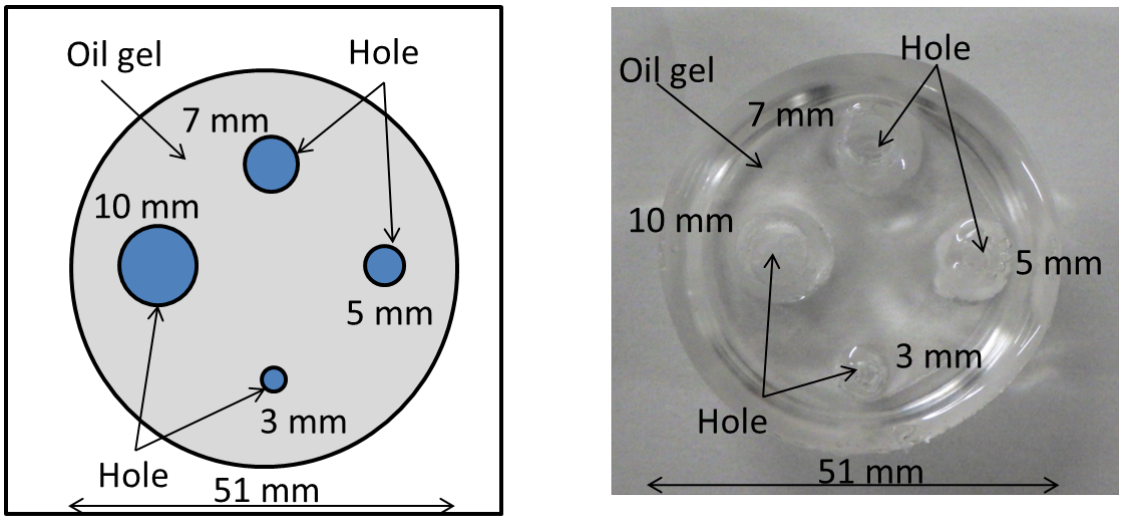

Figure 2. Sketch (left) and photograph (right) of the breast mimicking phantom with inclusions with diameter 3, 5, 7, and 10 mm.

[7] Li, C., Duric, N., and Huang, L., "Clinical breast imaging using sound-speed reconstructions of ultrasound tomography data," in [*Medical Imaging 2008: Ultrasonic Imaging and Signal Processing*], **6920**, 692009, International Society for Optics and Photonics (2008).
[8] Wiskin, J., Borup, D., Johnson, S., Andre, M., Greenleaf, J., Parisky, Y., and Klock, J., "Three-dimensional nonlinear inverse scattering: Quantitative transmission algorithms, refraction corrected reflection, scanner design and clinical results," in [*Proceedings of Meetings on Acoustics ICA2013*], **19**(1), 075001, ASA (2013).
[9] Malik, B., Klock, J., Wiskin, J., and Lenox, M., "Objective breast tissue image classification using quantitative transmission ultrasound tomography," *Scientific reports* **6**, 38857 (2016).
[10] Ozmen, N., Dapp, R., Zapf, M., Gemmeke, H., Ruiter, N. V., and van Dongen, K. W. A., "Comparing different ultrasound imaging methods for breast cancer detection," *IEEE transactions on ultrasonics, ferroelectrics, and frequency control* **62**(4), 637–646 (2015).
[11] van den Berg, P. M. and Abubakar, A., "Contrast source inversion method: State of art," *Progress in Electromagnetic Research* **34**, 189–218 (2001).
[12] Ramirez, A. B., Abreo, S. A., and van Dongen, K. W. A., "Selecting the number and location of sources and receivers for non-linear time-domain inversion," in [*2017 IEEE International Ultrasonics Symposium (IUS)*], 1–3, IEEE (2017).
[13] Virieux, J. and Operto, S., "An overview of full-waveform inversion in exploration geophysics," *Geophysics* **74**(6), WCC1–WCC26 (2009).
[14] Janssen, E., Taskin, U., and van Dongen, K. W. A., "Random frequency picking for waveform inversion," in [*Proceedings of Meetings on Acoustics ICU*], **38**(1), 020007, Acoustical Society of America (2019).
[15] Terada, T., Yamanaka, K., Suzuki, A., Tsubota, Y., Wu, W., and Kawabata, K.-i., "Highly precise acoustic calibration method of ring-shaped ultrasound transducer array for plane-wave-based ultrasound tomography," *Japanese Journal of Applied Physics* **56**(7S1), 07JF07 (2017).

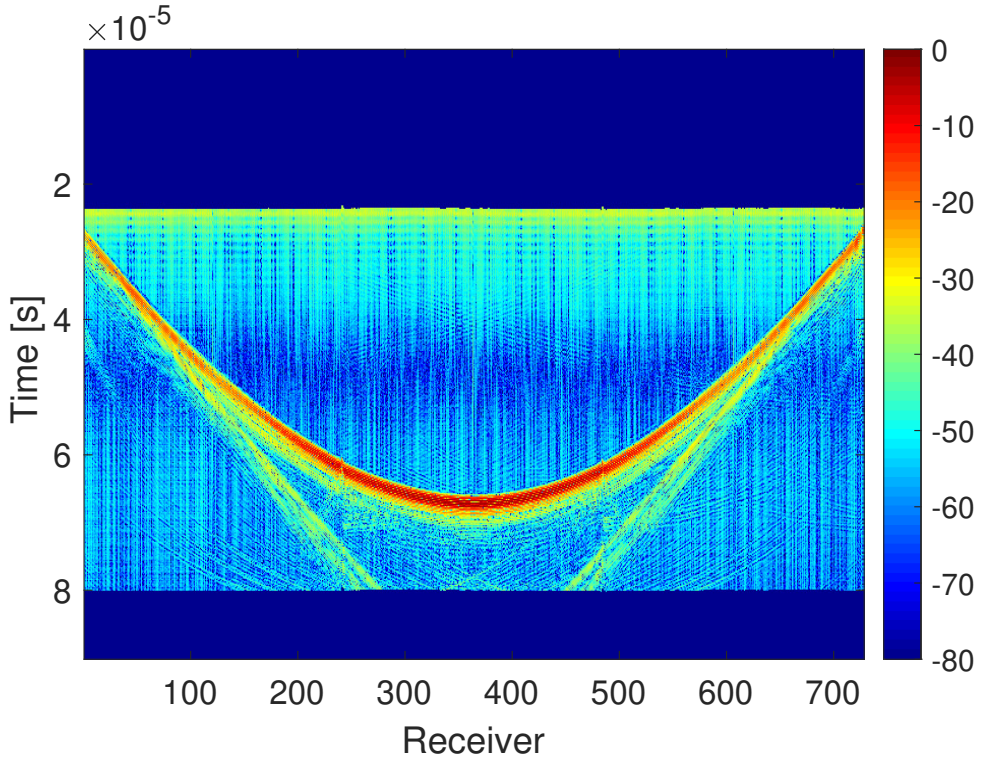

Figure 3. An example of a measured pressure field in dB in water for a single source and 768 receivers in time domain. Note that, the first part ($t < 2.3\ \mu s$) and the last part ($t > 8\ \mu s$) are suppressed as these parts were heavily contaminated with noise.

[16] Suzuki, A., Tsubota, Y., Wu, W., Yamanaka, K., Terada, T., and Kawabata, K., "Oil-gel-based phantom for mimicking wave refraction of breast in ultrasound computed tomography," in [*Medical Imaging 2018: Ultrasonic Imaging and Tomography*], Duric, N. and Byram, B. C., eds., **10580**, 149 – 154, International Society for Optics and Photonics, SPIE (2018).

[17] van den Berg, P., [*Forward and Inverse Scattering Algorithms Based on Contrast Source Integral Equations*], Wiley (2021).

[18] Taskin, U. and Van Dongen, K. W. A., "Multi-parameter inversion with the aid of particle velocity field reconstruction," *The Journal of the Acoustical Society of America* **147**(6), 4032–4040 (2020).

[19] Taskin, U., van der Neut, J., Gemmeke, H., and van Dongen, K. W. A., "Redatuming of 2-d wave fields measured on an arbitrary-shaped closed aperture," *IEEE transactions on ultrasonics, ferroelectrics, and frequency control* **67**(1), 173–179 (2019).

[20] Taskin, U. and van Dongen, K. W. A., "3d redatuming for breast ultrasound," in [*Medical Imaging 2020: Physics of Medical Imaging*], **11312**, 113125H, International Society for Optics and Photonics (2020).

[21] Taskin, U. and van Dongen, K. W. A., "A frequency-hopping technique for solving the cycle-skipping problem encountered with acoustic full-waveform inversion," in [*2020 IEEE International Ultrasonics Symposium (IUS)*], 1–3, IEEE (2020).

[22] Ramirez, A. B. and van Dongen, K. W. A., "Can sources and receivers be interchanged for imaging?," in [*2016 IEEE International Ultrasonics Symposium (IUS)*], 1–4, IEEE (2016).

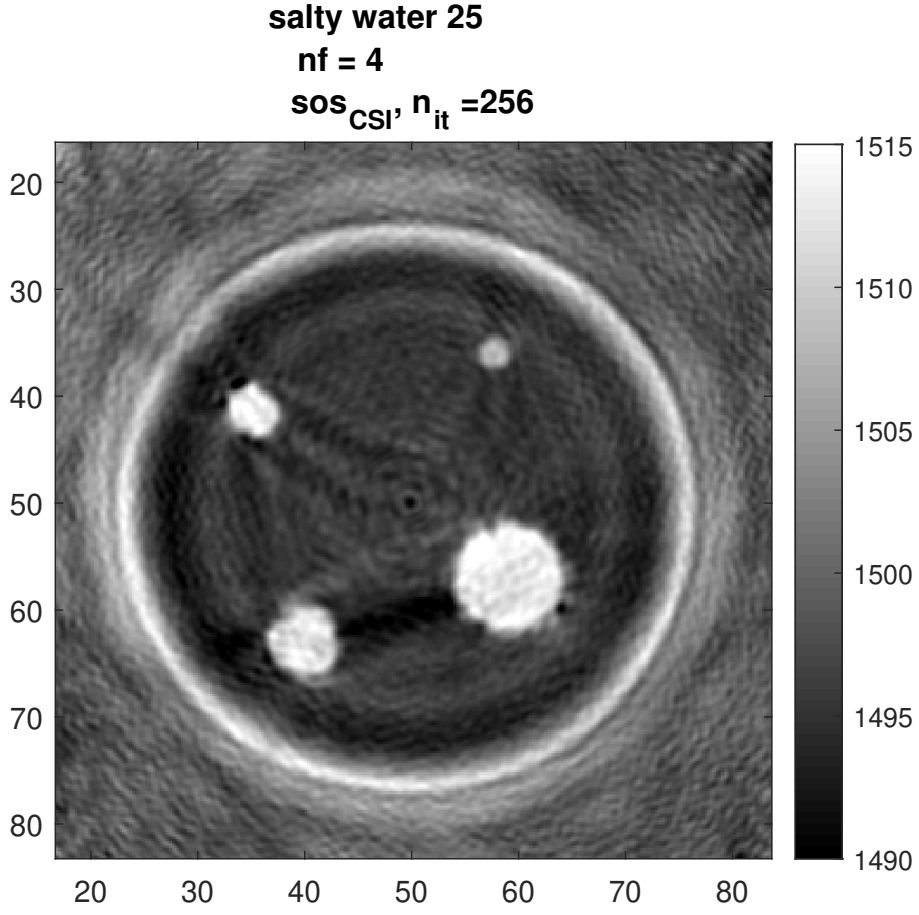

Figure 4. CSI result obtained with four frequency components after 256 iterations.

[23] Zhao, W., Wang, H., Gemmeke, H., Van Dongen, K. W. A., Hopp, T., and Hesser, J., "Ultrasound transmission tomography image reconstruction with a fully convolutional neural network," *Physics in Medicine & Biology* **65**(23), 235021 (2020).

[24] Ramirez, A. B. and Van Dongen, K. W. A., "Sparsity constrained contrast source inversion," *The Journal of the Acoustical Society of America* **140**(3), 1749–1757 (2016).

[25] Bouchan, T. G., Taskin, U., and Van Dongen, K. W. A., "Wavelet regularized born inversion," in [*2019 IEEE International Ultrasonics Symposium (IUS)*], 1855–1858, IEEE (2019).